ISSN 0038-0946, Solar System Research, 2018, Vol. 52, No. 6, pp. 505–517. © Pleiades Publishing, Inc., 2018.
Original Russian Text © A.T. Basilevsky, Yu.V. Skorov, S.F. Hviid, S.S. Krasilnikov, U. Mall, H.U. Keller, 2018, published in Astronomicheskii Vestnik, 2018, Vol. 52, No. 6, pp. 521–533.

# Lineaments on the Surface of the Consolidated Material of the Comet 67P/Churyumov–Gerasimenko Nucleus

**A. T. Basilevsky[a, b, *], Yu. V. Skorov[b], S. F. Hviid[c], S. S. Krasilnikov[a, b], U. Mall[b], and H. U. Keller[d]**

[a] *Vernadsky Institute of Geochemistry and Analytical Chemistry, Russian Academy of Sciences, Moscow, 119991 Russia*
[b] *Max Planck Institute for Solar System Research, Göttingen, 37077 Germany*
[c] *German Aerospace Center (DLR), Institute for Planetary Research, D 12489 Berlin, Germany*
[d] *Institute for Geophysics and Extraterrestrial Physics, TU Braunschweig, Braunschweig, 38106 Germany*
**e-mail: atbas@geokhi.ru*

Received May 31, 2018

**Abstract**—Morphologic analysis of the fragments (500 × 500 pixels) of images of comet 67P/Churyumov–Gerasimenko obtained with the OSIRIS camera for 18 regions, where the consolidated material is exposed on the surface, has been carried out. In terms of resolution, the images form a series from 0.04 to 1.29 m/pixel; consequently, the areas covered by these fragments vary from 400 to ~400000 $m^2$. In all of the regions, lineaments resembling tension fractures—several dozens of structures per region—are seen; and their number scarcely changes when passing from high-resolution images to lower-resolution ones. It is clear that relatively small lineaments cease to be reliably distinguished when the image resolution worsens, but the largest and well-defined ones remain observable, while the number of larger lineaments grows proportionally to the survey area increasing. Undoubtedly, this is an observational effect, which was demonstrated by examples with an artificially worsened resolution. However, on the other hand, this means that the tension fractures of the consolidated nucleus material represent a hierarchic population of smaller (meters long) to larger (decameters and longer) features. The lineaments seen in the analyzed fragments of images were counted, their lengths were measured, and the spacings (the mean distances between lineaments) and, from them, the depths of penetration of fractures into the nucleus material were estimated. It has been shown that the mean length of lineaments within each studied region depends on its area (which here correlates with the image resolution) and the depths of fracture penetration into the nucleus body depends on the mean length of lineaments. Both dependences are close to a power law. In the images of four regions covering the areas from 100000 to 400000 $m^2$ with a resolution of 0.66–1.29 m/pixel, the structures that look like layering or sheet jointing are seen in addition to fracture lineaments. The tension fractures are apparently formed due to seasonal and diurnal variations of the temperature, while the nature of the formation of the layer-like structures is not yet fully understood.

*Keywords:* comet, nucleus, consolidated material, lineament, fracture, spacing

**DOI:** 10.1134/S0038094618060011

## INTRODUCTION

Comet 67P/Churyumov-Gerasimenko (hereafter, 67P), which was an object of the *Rosetta* mission investigations in 2014–2016 (Taylor et al., 2017; see also http://sci.esa.int/rosetta/2279-summary), is now the best studied representative of this class of celestial bodies. It belongs to the Jupiter family, which is a group of short-period comets, whose orbit aphelia are near the orbit of this planet. The orbital period of comet 67P is 6.55 yr. The aphelion and perihelion of its orbit are 5.68 and 1.24 AU, respectively, and the period of rotation is 12.40 h (Taylor et al., 2017). The rotation axis of comet 67P is tilted 52° with respect to the perpendicular to its orbital plane (which is close to the ecliptic) in such a way that, for a larger part of its journey around the Sun, the northern part of the cometary nucleus faces the Sun, while the southern part sees the Sun only during the perihelion passage of the comet. Consequently, in the northern part of the nucleus, the summer is long but cold, while it is short and hot in the southern part. As was shown by Keller et al. (2017), this leads to the south-to-north seasonal transfer of the material mobilized in sublimation.

The nucleus of 67P is comprised of two lobes, which are informally called the Head and Body; and a relatively narrow part between them is called the Neck (Fig. 1). The sizes of the Head and Body lobes are 4.1 × 3.3 × 1.8 and 2.6 × 2.3 × 1.8 $km^3$, respectively (Sierks et al., 2015).

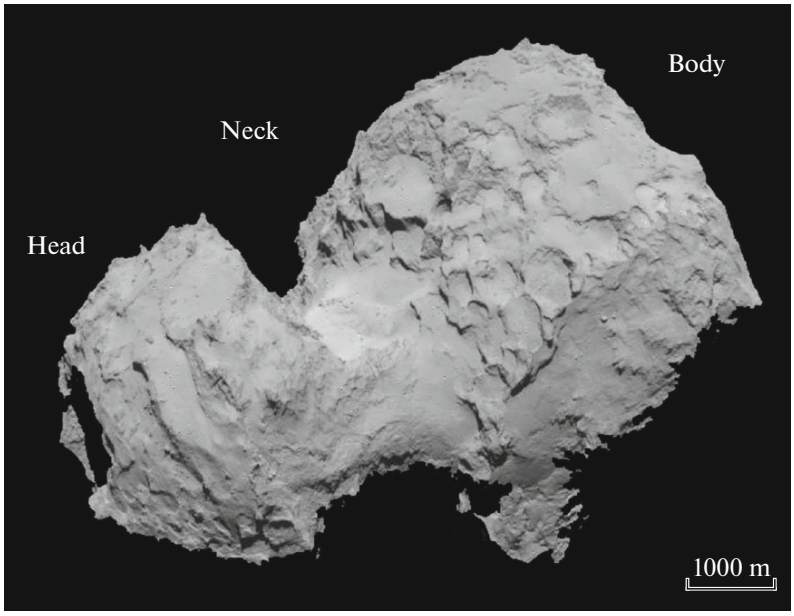


**Fig. 1.** The nucleus of comet 67P. Image ROS_CAM1_20140822T040718 taken by the *Rosetta* NavCam camera.

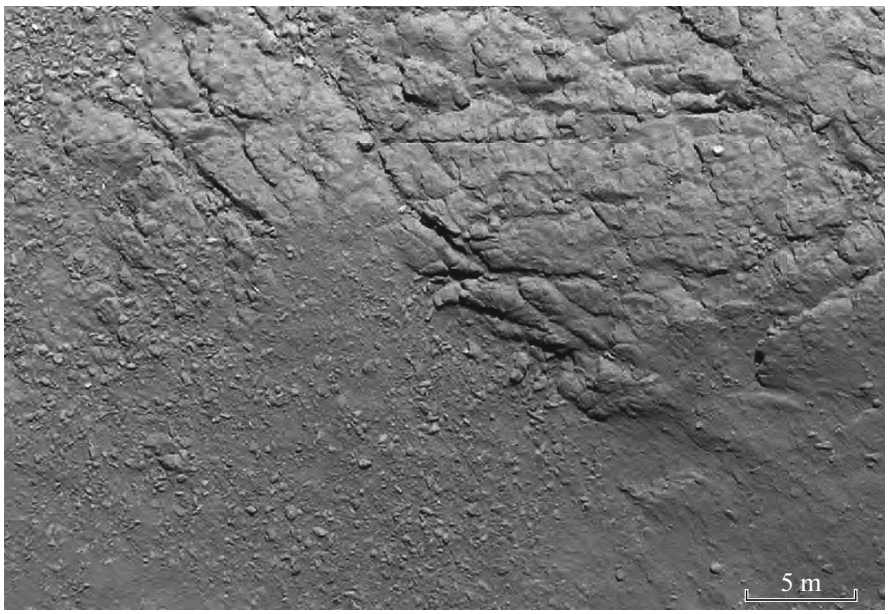


**Fig. 2.** The consolidated material of the 67P nucleus with fracture-like lineaments (top right) and the loose particulate material partly overlapping it (bottom left). A fragment of the OSIRIS image WAC_2016-09-30T10.28.37.743Z_IS20_1397549000_F12. The image resolution is 0.04 m.

The surface of the 67P nucleus is partly covered with the loose particulate material, from under which, here and there, the consolidated material is exposed (Fig. 2).

The loose material, the cometary regolith of a kind, is often called "airfall deposits" (e.g., Thomas et al., 2015), because this material, particle by particle, was dragged and elevated above the surface by the gas formed in sublimation of the near-surface ice. A part of this material, which was dragged by a gas flow, escaped to open space; and the other was deposited on the cometary surface as if from "air". In addition, a part of the loose surface material is formed in sublimational weathering of the consolidated nucleus material exposed on the slopes, falls down, and accumulates at the base of slopes as, for example, at the Hathor cliff base (Basilevsky et al., 2017).

**Table 1.** The images analyzed in the paper

| No | Region | Image number | Resolution, m/pixel | Location |
|---|---|---|---|---|
| 1 | 1 | NAC_2016-09-02T19.57.44.449Z_ID20_1397549001_F22 | 0.05 | Head |
| 2 | 2 | WAC_2016-09-30T10.28.37.743Z_IS20_1397549000_F12 | 0.05 | Head |
| 3 | 3 | NAC_2016-05-19T11.08.37.677Z_IS20_1397549000_F22 | 0.11 | Head |
| 4 | 4 | NAC_2016-09-08T23.28.34.739Z_IS20_1397549100_F22 | 0.04 | Body |
| 5 | 5 | NAC_2016-09-08T23.18.33.747Z_IS20_1397549600_F22 | 0.04 | Body |
| 6 | 6 | NAC_2016-09-05T21.38.03.522Z_ID10_1397549001_F41 | 0.05 | Body |
| 7 | 7 | NAC_2016-08-06T02.23.34.841Z_IS20_1397549900_F22 | 0.14 | Head |
| 8 | 8 | NAC_2016-07-30T12.58.59.641Z_IS20_1397549002_F41 | 0.15 | Head |
| 9 | 9 | NAC_2016-08-06T01.35.34.784Z_IS20_1397549100_F22 | 0.16 | Head |
| 10 | 10 | NAC_2016-08-03T07.48.34.765Z_ID20_1397549400_F22 | 0.15 | Body |
| 11 | 11 | NAC_2016-08-06T01.58.34.764Z_IS20_1397549500_F22 | 0.15 | Body |
| 12 | 12 | NAC_2016-05-11T09.36.28.969Z_ID20_1397549000_F22 | 0.16 | Body |
| 13 | 13 | NAC_2014-09-30T08.54.41.560Z_IS20_1397549700_F22 | 0.33 | Body |
| 14 | 14 | NAC_2014-09-29T17.29.17.542Z_IS20_1397549100_F22 | 0.34 | Head |
| 15 | 15 | NAC_2016-03-23T06.59.39.509Z_IS20_1397549200_F22 | 0.66 | Body |
| 16 | 16 | NAC_2016-02-07T08.25.51.483Z_IS20_1397549002_F22 | 0.86 | Body |
| 17 | 17 | NAC_2016-01-30T13.11.49.715Z_IS20_1397549500_F22 | 1.11 | Body |
| 18 | 18 | NAC_2016-01-27T16.20.08.963Z_IS20_1397549000_F22 | 1.29 | Head |

The consolidated material observed on the surface is apparently almost the same as that underneath (except the sublimational loss of volatiles, which is typical of the surface). According to Patzold et al. (2016), its density is 533 ± 6 kg/m$^3$, the porosity is 72–74%, and the dust-to-ice ratios by mass and volume are close to 4 and 2, respectively. The consolidated material is able to keep steep, vertical, and even negative slopes (see, e.g., Basilevsky et al., 2016; Groussin et al., 2015); and its surface often exhibits lineaments (Fig. 2; see also Thomas et al., 2015; El-Maarry et al., 2015; Auger et al., 2018).

In this paper, we study lineaments on the surface of the consolidated material of the 67P nucleus by attempting to estimate the depth of their penetration into the cometary nucleus on the basis of their typical length and spacing. For this, we analyze a sample of 18 images taken with the OSIRIS camera (Keller et al., 2007) for the surface regions of the cometary nucleus, within which the consolidated material is exposed. The image fragments of 500 × 500 pixels in size are examined. The resolution of these images ranges from 0.04 to 1.29 m/pixel (in the mentioned papers, the images with a resolution no better than 0.3 m were analyzed), which makes it possible to trace the changes observed or not observed with changing the resolution and, consequently, the sizes of the considered region. Moreover, within the bounds of possibility, we tried to compare the images of the regions on the Body to those for the Head. In the paper by Massironi et al. (2015) dealing with the orientation of the layer-like surface elements, it is concluded that earlier the lobes of comet 67P—the Body and the Head—were two independent bodies, which were joined together in a low-velocity collision. Comparison of structural peculiarities of the consolidated material of the Body and the Head of the nucleus, if it reveals essential differences between them, could serve as an additional argument for this hypothesis.

## THE SURFACE MORPHOLOGY OF ANALYZED SITES

Table 1 lists the images analyzed in this paper, their resolution, and the location of the observed regions in Body–Head terms; their concrete location on the cometary nucleus is shown in Fig. 3.

Figures 4 and 5 show the fragments of the images with a resolution of 0.04–0.34 and 0.66–1.29 m/pixel, respectively; and the same fragments with indicated lineaments are in Figs. 6–8.

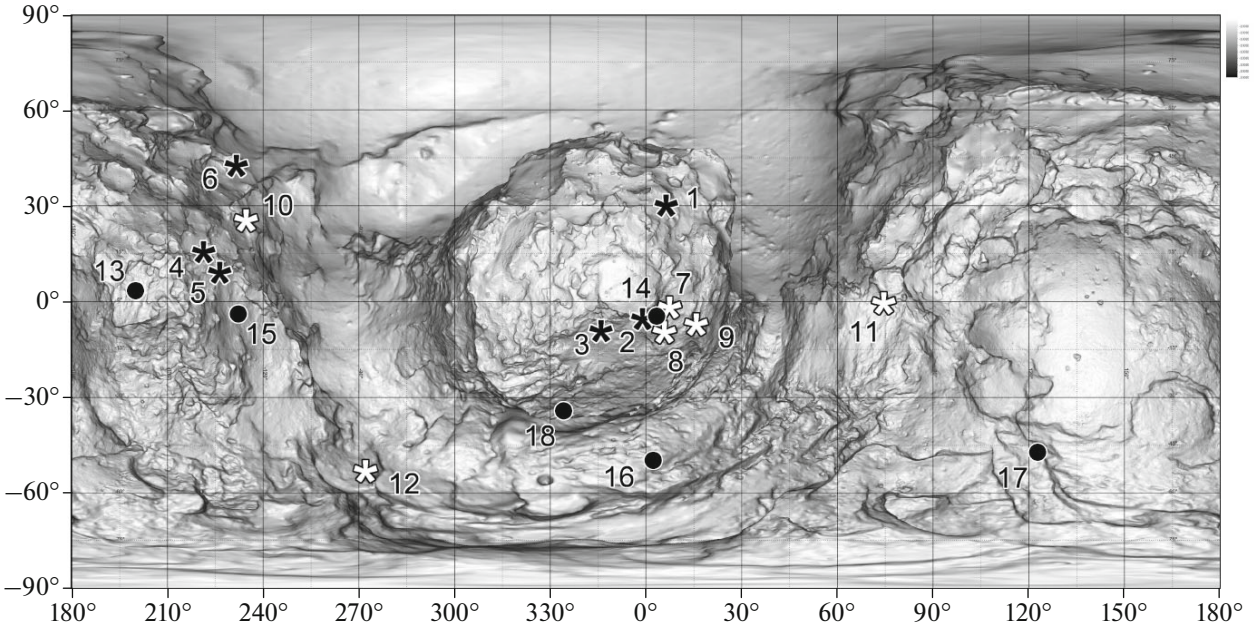


**Fig. 3.** Location of the analyzed regions on the map of the surface of the 67P nucleus. White stars, black stars, and black circles show the regions presented in the images with a resolution of 0.04–0.11, 0.14–0.16, and 0.33–1.29 m/pixel, respectively. The rounded feature of 30° × 30° in size seen in the center of the map is the Head of the nucleus.

It is seen in Figs. 4–8 that several tens of lineaments (from 23 to 97) are distinguishable in each of the fragments. Most lineaments are narrow (generally, less than 1 m in width) and rectilinear, and some of them are arched and resemble ruptures. In most cases, no prevailing directions of their orientation are observed; at the same time, in some regions, the predominance of two directions, or even one, is seen. However, it should be considered that the viewing directions were only rarely close to the local vertical; this circumstance should influence the observed orientation of lineaments and even the conditions for their visibility. We noticed no systematic differences between the regions on the Head and the Body of the nucleus in terms of the number or character of lineaments. We also found no systematic differences in the general character of lineaments with changing the image resolution from 0.04 to 0.34 m/pixel, when the covered areas increased from 400 to ~30000 $m^2$, respectively. However, in the images with a resolution of 0.66–1.29 m/pixel, which cover the areas from ~100000 to ~400000 $m^2$, the observed surface morphology changes: in addition to lineaments of the same type as those on higher-resolution images, the forms resembling layers or sheet jointing become to be seen. In Fig. 9, the images of probable terrestrial analogs of the discussed cometary lineaments are presented. Though the conditions on the cometary nucleus drastically differ from those on the Earth, probable analogies are widely considered in planetology (see, e.g., Auger et al. (2018) and Giacomini et al. (2016) for fractures and dunes, respectively).

When comparing the cometary lineaments (Figs. 4–8) to the terrestrial forms shown in Fig. 9, it is seen that the cometary lineaments observed in the images with a resolution of 0.04–0.34 m/pixel look like the terrestrial tension fractures, which was earlier mentioned by El-Maary et al. (2015). At the same time, in the images with a resolution of 0.66–1.29 m/pixel, in addition to the fracture-like lineaments, the forms resembling the terrestrial textures of sheeting, layering, and sheet jointing are seen. The presence of such structures on the 67P nucleus was earlier mentioned, for example, by Thomas et al. (2015) and Massironi et al. (2015).

In the course of the analysis, the numbers and the lengths of lineaments in 18 regions were measured; and the spacings and, consequently, the depths of penetration of fractures into the nucleus were estimated (Table 2). Since the lineaments intersect under different angles and the distances between them are not the same, the mean distance between them (the spacing) cannot be measured in a simple way. Consequently, some analog of the spacing was estimated. For this, the area of a considered region was divided by the number of lineaments in it; and the square root of the area per lineament was taken. In some degree, the obtained quantity is the estimate of the mean distance between lineaments, i.e., the spacing analog for the considered region. In its turn, assuming the lineaments to be ten-

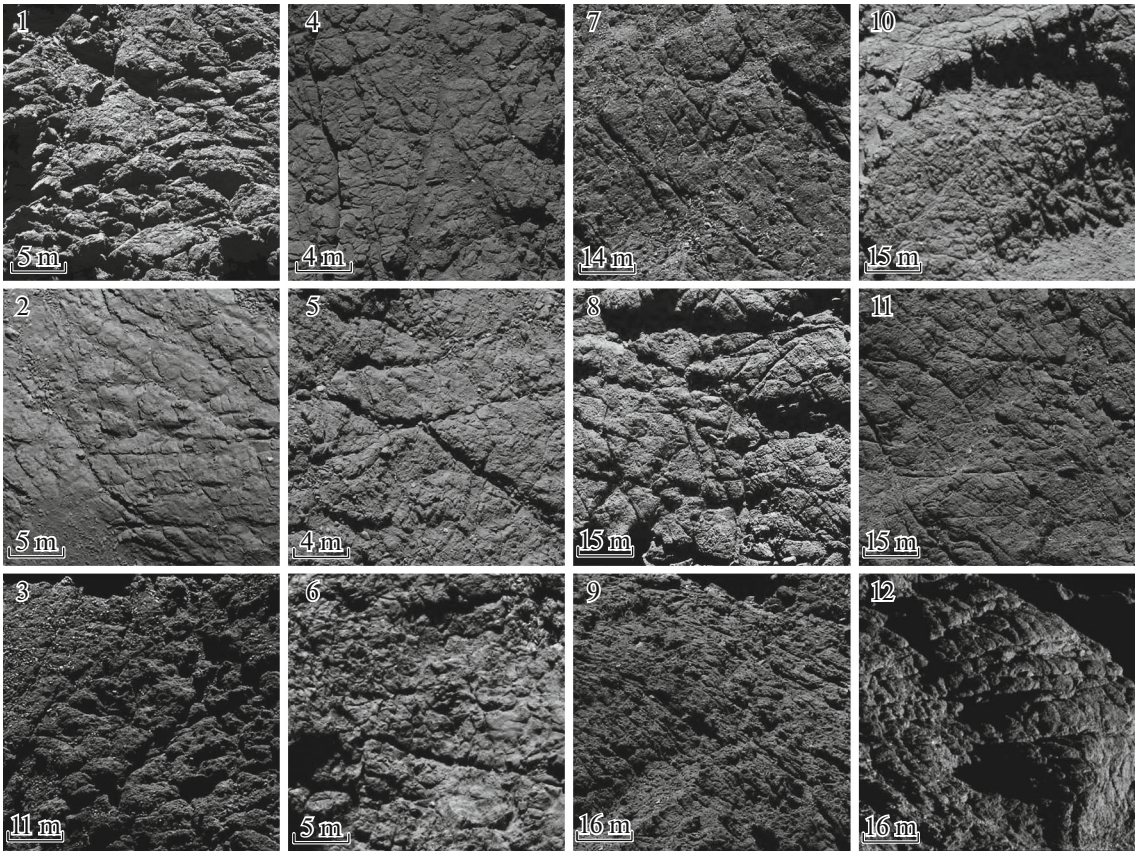


**Fig. 4.** Fragments (500 × 500 pixels) of the considered images with a resolution of 0.04–0.16 m/pixel. Regions 1–3 and 7–9 are on the Head of the nucleus, while regions 4–6 and 10–12 are on the Body. Such an arrangement of the fragments makes it easier to compare the surface morphology of the regions on the Head and the Body presented by the images of roughly the same resolution.

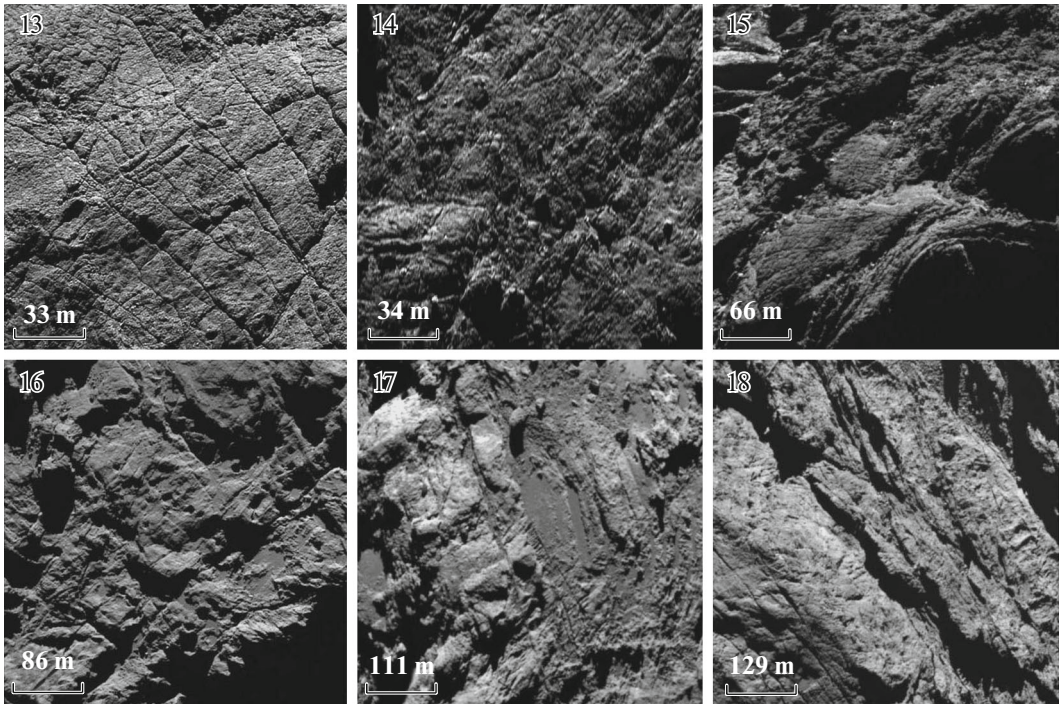


**Fig. 5.** Fragments (500 × 500 pixels) of the considered images with a resolution of 0.33–1.29 m/pixel. Regions 14 and 18 are on the Head of the nucleus, while regions 13, 15, 16, and 17 are on the Body.

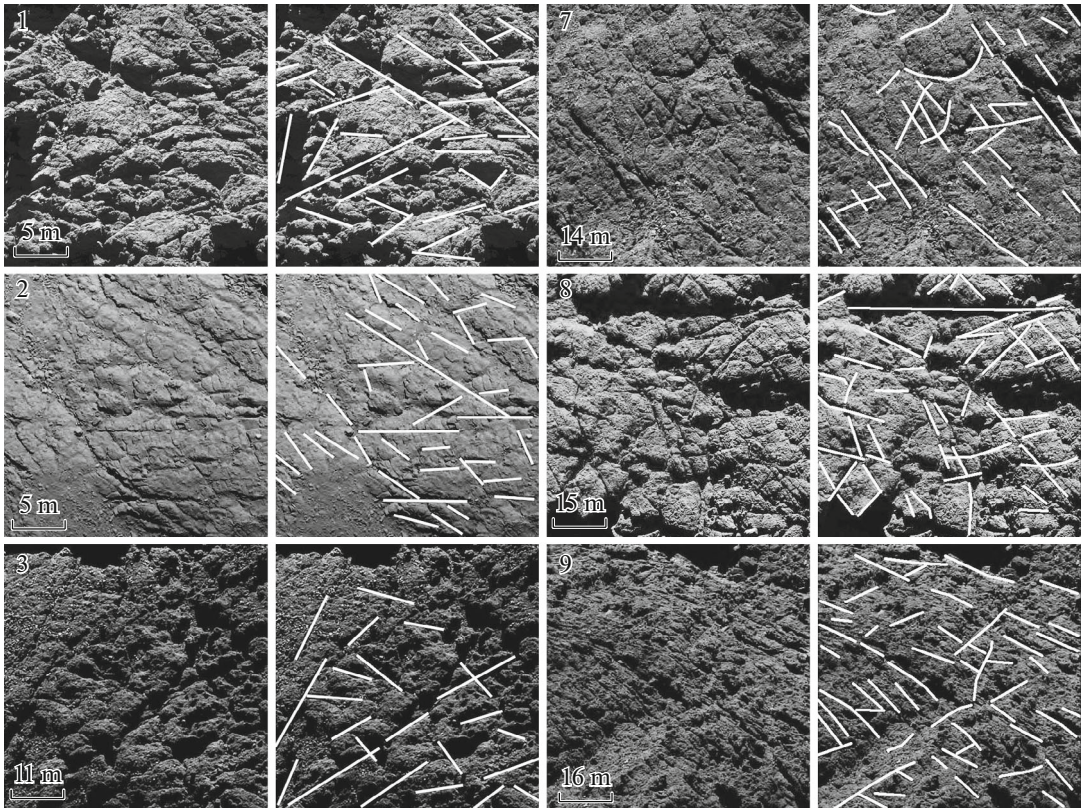


**Fig. 6.** Fragments of the images with a resolution of 0.05–0.16 m/pixel for the regions on the Head of the nucleus and the results of mapping the lineaments (while lines) in these regions.

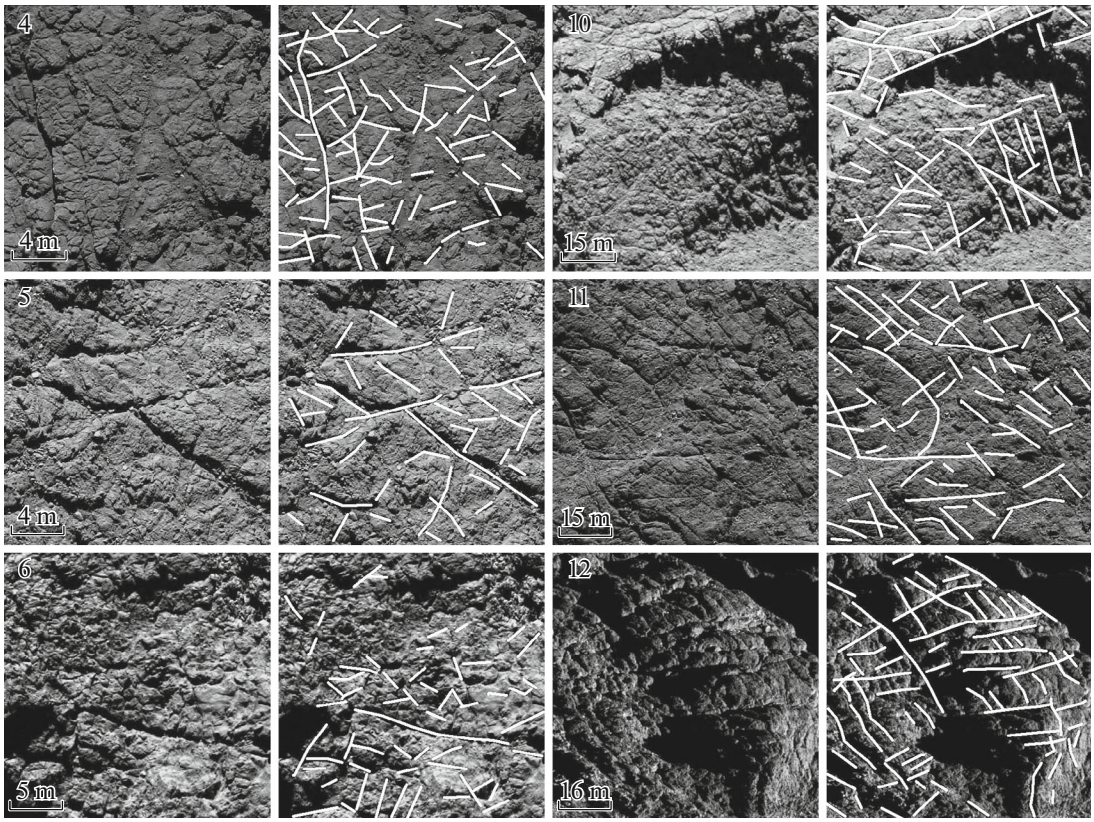


**Fig. 7.** Fragments of the images with a resolution of 0.05–0.16 m/pixel for the regions on the Body of the nucleus and the results of mapping the lineaments (white lines) in these regions.

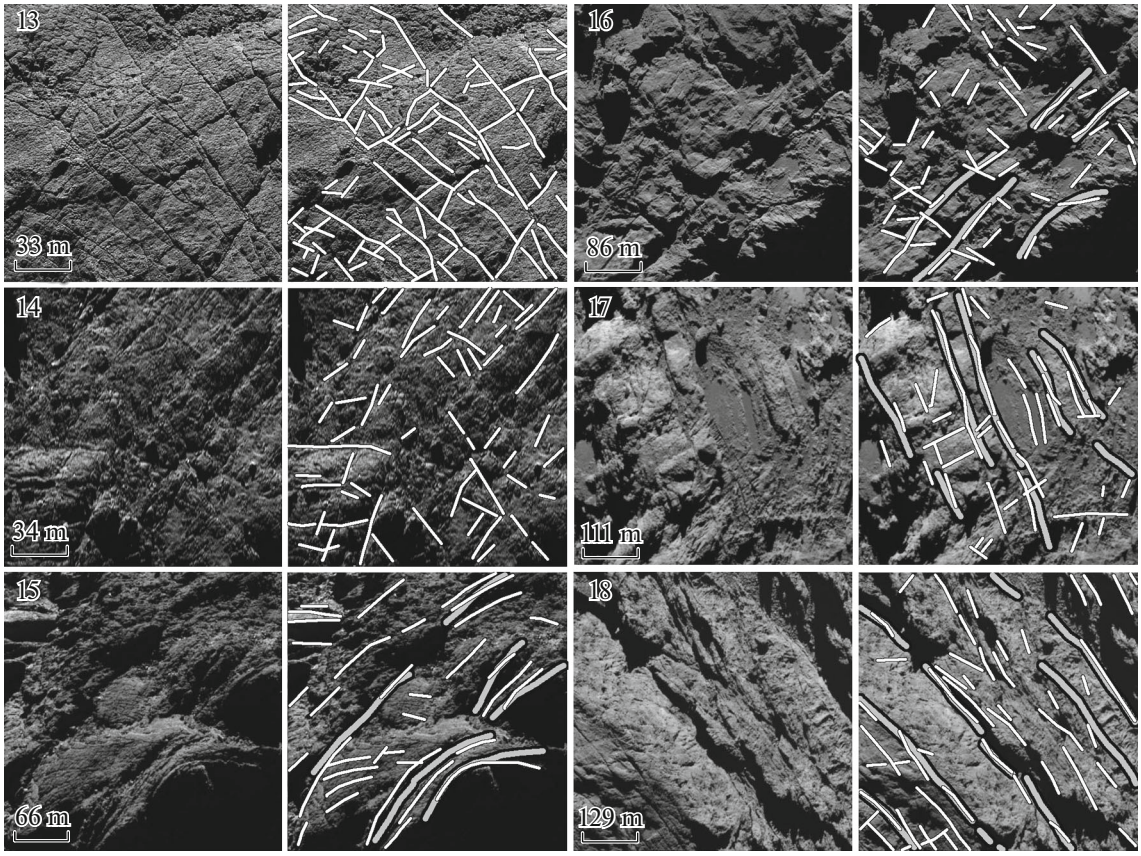


**Fig. 8.** Fragments of the images with a resolution of 0.33–1.29 m/pixel for the regions on the Head and the Body of the cometary nucleus and the results of mapping the lineaments in these regions. The fracture-like lineaments are shown with thin white lines. The structures resembling layers or sheet jointing are indicated by wider gray curves lightly edged black. Their lengths were not measured, and the spacings (see text) were not estimated.

sion fractures, we used these spacing values to estimate the depth of penetration of these fractures into the material of the nucleus. As follows from the results of Lachenbruch (1962), Corte and Higashi (1964), Neal et al. (1968), Parker (1999), Gudmundsson (1987), and El-Maarry et al. (2014), the penetration depth of fractures ranges from 1/10 to 1 of the spacing value; and the most probable value is usually accepted to be between 1/3 and 1/4. We use here a value of 1/3 (see Table 2). On the basis of the papers by Lachenbruch (1961) and Nur (1982), Gudmundsson (1987) points out that the penetration depth of fractures is approximately equal to or smaller than the fracture length. The data presented in Table 2 allow the results of our measurements and estimates to be compared.

From Figs. 4–8 and the results of measurements presented in Table 2, it is seen that, when the pixel size increases and, consequently, the area covered by a pixel increases, the number of observed lineaments remains almost the same, but their length systematically increases. It is evident that relatively small lineaments cannot be reliably distinguished when the image resolution worsens, but the largest and best-defined ones remain to be seen; at the same time, their number grows with increasing the observed area, and this number approximately corresponds to the number of smaller lineaments distinguishable in the higher-resolution images. On the one hand, this is an observational effect, which is demonstrated in Figs. 10 and 11. On the other hand, this means that the lineaments of the consolidated nucleus material, apparently corresponding to fractures, represent a hierarchically organized population of small (meters) to larger (tens of meters and more) forms.

The dependence of the mean length of deciphered lineaments on the area of the considered regions, which correlates with the image resolution in this case, is shown in panel *1* of Fig. 12, while the estimate of the depth of penetration of fractures into the nucleus material versus the mean length of the deciphered lineaments is shown in panel *2* of Fig. 12.

It is seen from Fig. 12 (panel *1*) that the mean length of lineaments in the regions regularly grows when then the area of the studied regions increases,


**Fig. 9.** Terrestrial forms resembling the discussed lineaments on the 67P nucleus surface: (1) tension fractures in basalts of the Isle of Skye, Scotland (https://tangledfrog.deviantart.com/art/Cracked-Rocks-179913174, UK); (2) tension fractures in greywackes of Virginia (https://whatterockstellus.blogspot.ru/2012/03/dominoes-anyone.html); (3) shear fractures in basalts of the Glengarry Basin, Australia (https://en.wikipedia.org/wiki/Shear_(geology)#media/File:Asymmetric_shear.jpg); (4) the layering in pyroclastic deposits, Eifel, Germany (https://www.alexstrekeisen.it/wulc/piroclastica.php); (5) the layering in the Toadstool sandstones, Nebraska, United States (https://academic.emporia.edu/aberjame/student/abel1/ground7.jpg; (6) the sheet jointing in granites, the Urals, Russia (https://naurale.com/items/1294).

which is accompanied by the resolution worsening in the considered cases; and this regularity well describes the data for the artificial worsening of the resolution (Figs. 10 and 11). From the results shown in Fig. 12 (panel *2*), it is seen that, when the mean length of the lineaments, which are apparently fractures, increases, the depth of penetration of these fractures into the body of the nucleus naturally increases. It is important to note that the data shown in the plots of Fig. 12 (panels *1* and *2*) for lineaments on the Head and the Body of the nucleus form a single sequence. In regions 15–18 shown in Figs. 5 and 8, the layer-type structures are seen. They are larger than fracture-like lineaments, and their nature may be different. Their depths of penetration into the nucleus have not been estimated. Probably, they are larger than those for fractures.

## DISCUSSION

In the previous section, the results of the morphologic analysis of the fragments (500 × 500 pixels) of the images of comet 67P/Churyumov–Gerasimenko obtained with the OSIRIS camera for 18 regions of the surface have been presented (Table 1 and Fig. 3). In these regions, the consolidated material of the nucleus is exposed on the surface. The resolution of the images is within the range from 0.04 to 1.29 m/pixel; consequently, the areas covered by these fragments vary from 400 to ~400000 m$^2$. In the studied regions, the lineaments resembling tension fractures are seen (Figs. 4–8). In each of the regions, there are several dozen lineaments; and their number scarcely changes when passing from high-resolution images to those of lower resolution. As noted above, the fact is that the relatively small lineaments cease to be reliably distinguishable when the image resolution worsens, but the largest and well-defined ones remain observable, while their number grows with the simultaneously increasing area observed. Undoubtedly, this is an observational effect, which was shown by examples in Figs. 10 and 11. However, on the other hand, this means that the lineaments of the consolidated nucleus material, which are apparently tension fractures, represent a hierarchically organized population of small (meters) to larger (decameters and longer) forms.

**Table 2.** The results of measurements of the number and the length of lineaments and the estimates of the spacing and the penetration depth of fractures (the columns are the line number (1), the region number (2), the image resolution (expressed in meters per pixel) (3), the region area (square meters) (4), the number of lineaments in the region (5), the scattering in the lineament length values in the region (meters) (6), the mean value of the lineament length (meters) (7), the standard deviation (8), the area per one lineament (squared meters) (9), the spacing (meters) (10), and the penetration depth of fractures (meters) (11)

| 1 | 2 | 3 | 4 | 5 | 6 | 7 | 8 | 9 | 10 | 11 |
|---|---|---|---|---|---|---|---|---|---|---|
| 1 | 1 | 0.05 | 625 | 32 | 2.35–17.7 | 5.53 | 3.31 | 19.5 | 4.4 | 1.5 |
| 2 | 2 | 0.05 | 625 | 40 | 2.4–19.45 | 4.35 | 2.95 | 15.6 | 3.9 | 1.3 |
| 3 | 3 | 0.11 | 3025 | 23 | 6.93–22.7 | 11.6 | 4.7 | 131 | 11 | 3.8 |
| 4 | 4 | 0.04 | 400 | 89 | 1.04–15.5 | 2.42 | 1.65 | 4.5 | 2.1 | 0.7 |
| 5 | 5 | 0.04 | 400 | 44 | 1.28–12.8 | 3.23 | 2.22 | 9.1 | 3.0 | 1.0 |
| 6[1] | 5* | 0.16 | 6400 | 79 | 2.88–34.7 | 9.2 | 5.5 | 81 | 9.0 | 3.0 |
| 7 | 6 | 0.05 | 625 | 57 | 1.15–15.6 | 2.8 | 1.96 | 10.9 | 3.3 | 1.1 |
| 8 | 7 | 0.14 | 4900 | 39 | 4.76–32.5 | 12.2 | 6.13 | 125 | 11 | 3.7 |
| 9 | 8 | 0.15 | 5625 | 47 | 5.25–61.6 | 12.6 | 8.64 | 120 | 10.9 | 3.6 |
| 10 | 9 | 0.16 | 6400 | 55 | 5.28–28.8 | 12.2 | 5.1 | 116 | 10.8 | 3.6 |
| 11 | 10 | 0.15 | 5625 | 66 | 3.75–53.3 | 10.9 | 8.02 | 85 | 9.2 | 3.0 |
| 12 | 11 | 0.15 | 5625 | 77 | 4.05–33.0 | 10.7 | 5.9 | 73 | 8.5 | 2.8 |
| 13[1] | 11* | 0.60 | 90000 | 89 | 12.0–78.0 | 30.8 | 13.6 | 1011 | 31.8 | 10.6 |
| 14 | 12 | 0.16 | 6400 | 73 | 3.36–43.8 | 11.8 | 8.0 | 88 | 9.4 | 3.1 |
| 15 | 13 | 0.33 | 27225 | 97 | 4.95–75.9 | 20.3 | 12.8 | 281 | 16.8 | 5.6 |
| 16 | 14 | 0.34 | 28900 | 59 | 7.14–67.3 | 20.9 | 10.6 | 490 | 22.1 | 7.4 |
| 17 | 15 | 0.66 | 108900 | 35 | 26.4–148 | 61.4 | 31.3 | 3111 | 55.8 | 18.6 |
| 18 | 16 | 0.86 | 184900 | 62 | 21.5–117 | 44.2 | 19.7 | 2982 | 54.6 | 18.2 |
| 19 | 17 | 1.11 | 308025 | 43 | 21.1–324 | 72.8 | 51.1 | 7163 | 84.6 | 28.2 |
| 20 | 18 | 1.29 | 416025 | 49 | 24.5–233 | 89.8 | 45.8 | 8490 | 92.1 | 30.7 |

[1] The images with artificially worsened resolution were used for regions 5* and 11* (see text and Figs. 10 and 11).

In the studied fragments, the lineaments were counted (their numbers range from 23 to 97), their lengths were measured (from 2.4 to 90 m), and their spacings (the mean distances between lineaments) were estimated (from 2 to 90 m); from the latter quantity, the depths of penetration of lineaments into the nucleus material were found (from 0.7 to 30 m). The mean length of lineaments in a region versus the region area, which in turn depends on the image resolution, and the depth of penetration of fractures into the nucleus material versus the mean length of lineaments are shown in panels *1* and *2* of Fig. 12, respectively. Both dependences are clearly expressed and close to a power law. They agree well with the dependences for the fractures on the Earth and Mars (Lachenbruch, 1961; 1962; Corte and Higashi, 1964; Neal et al., 1968; Nur, 1982; Parker, 1999; Gudmundsson, 1987; El-Maarry et al., 2014). The data for lineaments on the Head and the Body shown in the plots of Fig. 12 (panels *1* and *2*) form a single sequence. Together with the above-noted external similarity of the lineaments, this fact suggests that they do not differ much. Our data do not support the hypothesis proposed by Massironi et al. (2015) that the Head and the Body were formed independently and were assembled into a single nucleus later; however, our data do not contradict it either.

As the comparison to the images of the terrestrial fractures (Fig. 9) shows, the discussed lineaments of the cometary nucleus are likely to be tension fractures, which is also consistent with the results by El-Maarry et al. (2015). Most probably, these fractures were formed due to diurnal and seasonal variations in the surface temperature of the nucleus. From the *Rosetta* data about the effective density of the surface material on the 67P nucleus (470 kg/m$^3$) and the thermal inertia (10–30 J/m$^2$ K s$^{1/2}$), Skorov et al. (2016) showed that the penetration depth of the seasonal thermal wave into the nucleus body is several meters. The diurnal wave penetrates into the depth that is 1.5–2 orders of magnitude smaller. From these estimates and taking into account the data on the penetration depth of fractures (Table 2), it follows that the lineaments of the

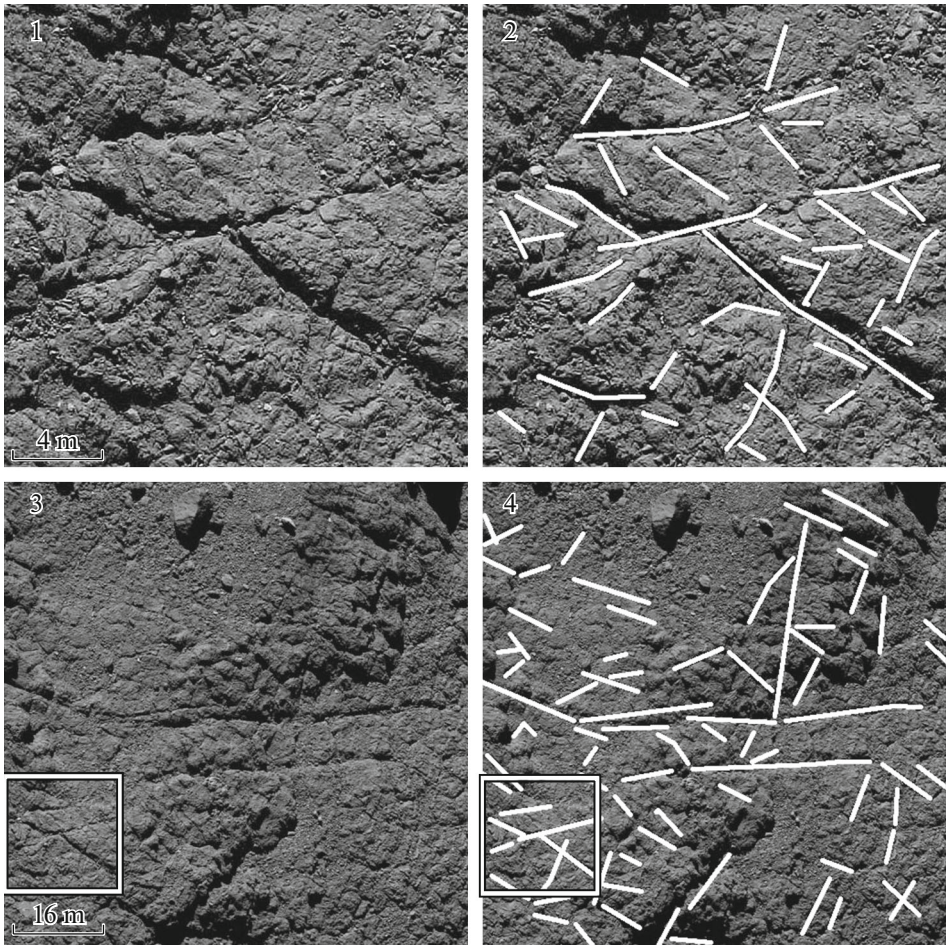


**Fig. 10.** The influence of the image resolution on identification of lineaments shown by an example of region 5: the fragment (500 × 500 pixels) of the NAC_2016-09-08T23.18.33.747Z_IS20_1397549600_F22 image with a resolution of 0.04 m/pixel (1); the same fragment with deciphered lineaments (2); the whole NAC_2016-09-08T23.18.33.747Z_IS20_1397549600_F22 image, the resolution of which was worsened to 0.16 m/pixel (3); the same image with deciphered lineaments (4).

type described are apparently actual tension fractures. In the images characterizing regions 1–14, the observed lineaments, which penetrate to depths of less than 10 m (according to our estimates), appear to be actually formed due to the temperature changes of the nucleus surface. However, the lineaments (fractures), which are observed in the images for regions 15–18 and penetrate to a depth of 20–30 m, are probably different in nature; they may be also of thermal origin but formed under different conditions of heating and cooling.

In the images of regions 15–18, covering the areas from 100000 to 400000 $m^2$ with a resolution of 0.66–1.29 m/pixel, the structures that look like the layering or sheet jointing are seen in addition to the fracture-type lineaments. As has been mentioned above, such features on the nucleus of comet 67P were described in several papers (e.g., Thomas et al., 2015; Massironi et al., 2015). Similar features were observed on the nuclei of comets 9P/Tempel 1 (A'Hearn et al., 2005; Thomas et al., 2007, 2013), 81P/Wild 2 (Brownlee et al., 2004), and 19P/Borrelly (Britt et al., 2004). Their origin is thought to be connected with the upflow of fluidized material (Belton and Melosh, 2009) or the primary accretion of cometary material (Belton et al. 2007; Lasue et al., 2009) during the so-called plantation of cometesimals that collided with the growing nucleus (see Basilevsky and Keller, 2007, Fig. 8). On the 67P nucleus, the length of such structures is larger than a few hundred meters; and it is not clear whether their length and the depth of penetration into the nucleus material are connected.

## CONCLUSIONS

It follows from the above that lineaments of at least two types are observed on the surface of outcrops of the consolidated nucleus material of comet 67P: (1) the structures that are probably tension fractures

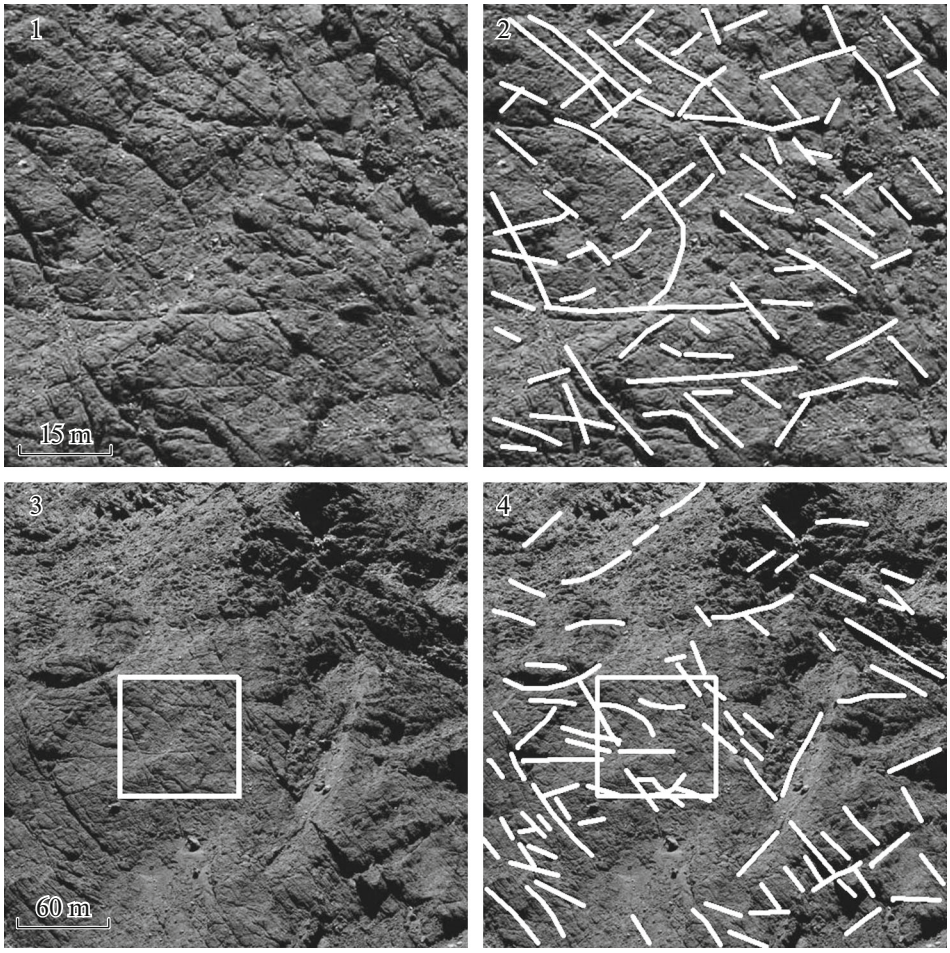


**Fig. 11.** The influence of the image resolution on identification of lineaments shown by an example of region 11: the fragment (500 × 500 pixels) of the NAC_2016-08-06T01.58.34.764Z_IS20_1397549500_F22 image with a resolution of 0.15 m/pixel (1); the same fragment with deciphered lineaments (2); the whole NAC_2016-08-06T01.58.34.764Z_IS20_1397549500_F22 image, the resolution of which was worsened to 0.60 m/pixel (3); the same image with deciphered lineaments (4).

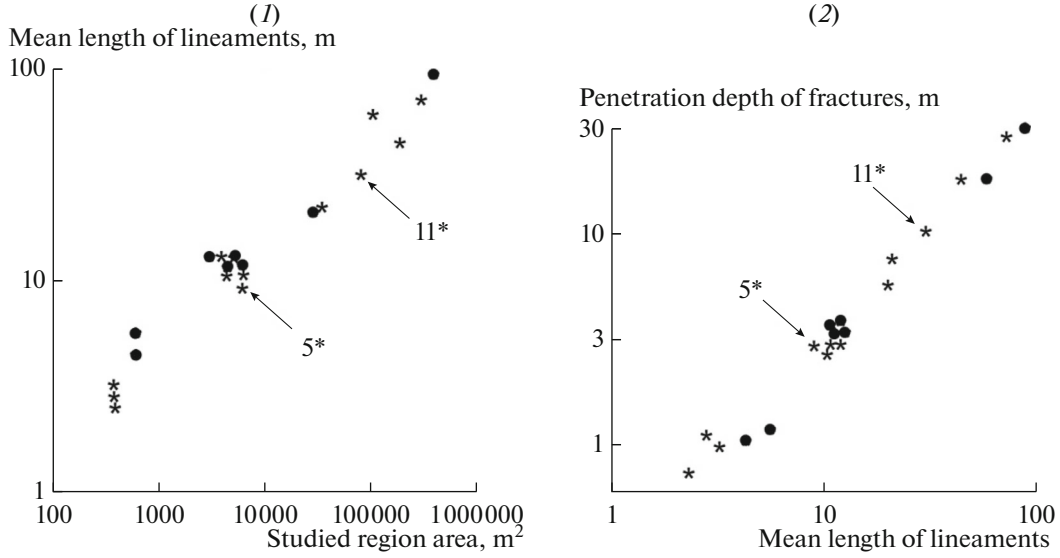


**Fig. 12.** The mean length of deciphered lineaments in dependence on the area of considered regions (which correlates with the image resolution) (panel *1*) and the depth of penetration of fractures into the nucleus material in dependence on the mean length of deciphered lineaments (panel *2*). The data for lineaments on the Head and the Body are shown by black circles and stars, respectively.

and (2) the layer-type structures. It is likely that most lineaments of the first type, whose depth of penetration into the nucleus material is less than 10 m, resulted from seasonal (and diurnal) temperature changes in the surface temperature; and they form a hierarchically organized population. The layer-type structures probably appeared very early, and the details of their origin are under discussion.

## ACKNOWLEDGMENTS

The authors would like to thank B.A. Ivanov for useful comments which resulted in a much-improved paper.

This work was partially performed within the Program I.28 of Presidium of Russian Academy of Sciences, theme 0137-2018-0038 and the Max Planck Institute for Solar System Research (A.T. Bazilevsky and S.S. Krasilnikov). Yu.S. Skorov is grateful to Deutsche Forschungsgemeinschaft (DFG), grant no. SK 264/1-1.

## REFERENCES

A'Hearn, M.F., Belton, M.G.S., Delamere, W.A., Kissel, J., Klaasen, K.P., McFadden, L.A., Meech, K.J., Melosh, H.J., Schultz, P.H., Sunshine, J.M., and 22 coauthors, Deep impact: excavating comet Tempel 1, *Science,* 2005, vol. 310, pp. 258–264. doi 10.1126/science.1118923

Auger, A.-T., Groussin, O., Jorda, L., El-Maarry, M.R., Bouley, S., Séjourné, A., Gaskell, R., Capanna, C., Davidsson, B., Marchi, S., and 41 coauthors, Meter-scale thermal contraction crack polygons on the nucleus of comet 67P/Churyumov-Gerasimenko, *Icarus,* 2018, vol. 301, pp. 173–188. doi 10.1016/j.icarus.2017.09.037

Basilevsky, A.T. and Keller, H.U., Craters, smooth terrains, flows, and layering on the comet Nuclei, *Sol. Syst. Res.,* 2007, vol. 41, no. 2, pp. 109–117. doi 10.1134/S0038094607020037

Basilevsky, B.T., Krasil'nikov, S.S., Shiryaev, A.A., Mall, U., Keller, H.U., Skorov, Yu.V., Mottola, S., and Hviid, S.F., Estimating the strength of the nucleus material of comet 67P Churyumov-Gerasimenko, *Sol. Syst. Res.,* 2016, vol. 50, no. 4, pp. 225–234. doi 10.1134/S0038094616040018

Basilevsky, A.T., Mall, U., Keller, H.U., Skorov, Yu.V., Hviid, S.F., Mottola, S., Krasilnikov, S.S., and Dabrowski, B., Geologic analysis of the Rosetta NavCam, Osiris and ROLIS images of the comet 67P/Churyumov-Gerasimenko nucleus, *Planet. Space Sci.,* 2017, vol. 137, pp. 1–19. doi 10.1016/j.pss.2017.01.002

Belton, M.J.S., Thomas, P., Veverka, J., Schultz, P., A'Hearn, M.F., Feaga, L., Farnham, T., Groussin, O., Li, J.-Ya., Lisse, C., McFadden, L., Sunshine, J., Meech, K.J., Delamere, W.A., and Kissel, J., The internal structure of Jupiter family cometary nuclei from Deep Impact observations: the "talps" or "layered pile" model, *Icarus,* 2007, vol. 187, pp. 332–344. doi 10.1016/j.icarus.2006.09.005

Belton, M.J.S. and Melosh, J., Fluidization and multiphase transport of particulate cometary material as an explanation of the smooth terrains and repetitive outbursts on 9P/Tempel 1, *Icarus,* 2009, vol. 200, pp. 280–291. doi 10.1016/j.icarus.2008.11.012

Britt, D.T., Boice, D.T., Buratti, B.J., Campins, N., Nelson, R.M., Oberst, J., Sandel, B.R., Stern, S.A., Soderblom, L.A., and Thomas, N., The morphology and surface processes of comet 19/P Borrelly, *Icarus,* 2004, vol. 167, pp. 45–53. doi 10.1016/j.icarus.2003.09.004

Brownlee, D.E., Horz, F., Newburn, R.L., Zolensky, M., Duxbury, T.C., Sandford, S., Sekanina, Z., Tsou, P., Hanner, M.S., Clark, B.C., Green, S.F., and Kissel, J., Surface of young Jupiter family comet 81P/Wild 2: view from the Stardust spacecraft, *Science,* 2004, vol. 304, pp. 1764–1769. doi 10.1126/science.1097899

Corte, A. and Higashi, A., *Experimental Research on Desiccation Cracks in Soil: Research Report No. 66*, Wilmette, Ill: US Army Snow, Ice Permafrost Res. Establishment, 1964, p. 72.

El-Maarry, M.R., Watters, W., McKeown, N.K., Carter, J., Noe Dobrea, E., Bishop, J.L., Pommerol, A., and Thomas, N., Potential desiccation cracks on Mars: a synthesis from modeling, analogue-field studies, and global observations, *Icarus,* 2014, vol. 241, pp. 248–268. doi 10.1016/j.icarus.2014.06.033

El-Maarry, M.R., Thomas, N., Gracia-Bern, A., Marschall, R., Auger, A.-T., Groussin, O., Mottola, S., Pajola, M., Massironi, M., Marchi, S., et al.,, Fractures on comet 67P/Churyumov-Gerasimenko observed by Rosetta/OSIRIS, *Geophys. Rev. Lett.,* 2015, vol. 42, no. 13, pp. 5170–5178. doi 10.1002/2015GL064500

Giacomini, L., Massironi, M., El-Maarry, M.R., Penasa, L., Pajola, M., Thomas, N., Lowry, S.C., Barbieri, C., Cremonese, G., Ferri, F., and 46 coauthors, Geologic mapping of the comet 67P/Churyumov-Gerasimenko's northern hemisphere, *Mon. Not. R. Astron. Soc.,* 2016, vol. 462, pp. S352–S367. doi 10.1093/mnras/stw2848

Groussin, O., Jorda, L., Auger, A.-T., Kührt, E., Gaskell, R., Capanna, C., Scholten, F., Preusker, F., Lamy, P., Hviid, S., and 42 coauthors, Gravitational slopes, geomorphology and material strengths of the nucleus of comet 67P/Churyumov-Gerasimenko from OSIRIS observations, *Astron. Astrophys.,* 2015, vol. 583, pp. 1–12. doi 10.1051/0004-6361/201526379

Gudmundsson, A., Geometry, formation and development of tectonic fractures on the Reykjanes Peninsula, Southwest Iceland, *Tectonophysics,* 1987, vol. 139, pp. 295–308. doi 10.1016/0040-1951(87)90103-X

Keller, H.U., Lamy, P., Rickman, H., Rodrigo, R., Wenzel, K.-P., Sierks, H., A'Hearn, M.F., Angrilli, F., Angulo, M., and 59 coauthors, OSIRIS – the scientific camera system onboard Rosetta, *Space Sci. Rev.,* 2007, vol. 128, pp. 433–506. doi 10.1007/s11214-006-9128-4

Keller, H.U., Mottola, S., Hviid, S.F., Agarwal, J., Kührt, E., Skorov, Y., Otto, K., Vincent, J.-B., Oklay, N., Schröder, S.E., and 40 coauthors, Seasonal mass transfer on the nucleus of comet 67P/Chuyumov-Gerasimenko, *Mon. Not. R. Astron. Soc.,* 2017, vol. 469, suppl. 2, pp. S357–S371. doi 10.1093/mnras/stx1726

Lachenbruch, A.H., Depth and spacing of tension cracks, *J. Geophys. Res.,* 1961, vol. 66, no. 12, pp. 4273–4292. doi 10.1029/JZ066i012p04273

Lachenbruch, A.H., *Mechanics of thermal contraction cracks and ice-wedge polygons in permafrost*, *Geol. Soc. Am. Spec. Pap.,* 1962, vol. 70, pp. 1–66. http://specialpapers.gsapubs.org/content/70/1.full.pdf+html. doi 10.1130/SPE70-p1

Lasue, J., Botet, R., Levasseur-Regourd, A.C., and Hadamcik, E., Cometary nuclei internal structure from early aggregation simulations, *Icarus,* 2009, vol. 203, pp. 599–609. doi 10.1016/j.icarus.2009.05.013

Massironi, M., Simioni, E., Marzari, F., Cremonese, G., Giacomini, L., Pajola, M., Jorda, L., Naletto, G., Lowry, S., El-Maarry, M.R., and 50 coauthors, Two independent and primitive envelopes of the bilobate nucleus of comet 67P, *Nature,* 2015, vol. 526, pp. 402–405. doi 10.1038/nature15511

Neal, J.T., Langer, A.M., and Kerr, P.F., Giant desiccation polygons of Great Basin Playas, *Geol. Soc. Am. Bull.,* 1968, vol. 79, no. 1, p. 69. doi 10.1130/0016-7606(1968)79[69:GDPOGB]2.0.CO;2

Nur, A., The origin of tensile fracture lineaments, *J. Struct. Geol.,* 1982, vol. 4, pp. 31–40. doi 10.1016/0191-8141(82)90004-9

Parker, A.P., Stability of arrays of multiple edge cracks, *Eng. Fract. Mech.,* 1999, vol. 62, no. 6, pp. 577–591. doi 10.1016/S0013-7944(98)00110-6

Sierks, H., Barbieri, C., Lamy, P.L., Rodrigo, R., Koschny, D., Rickman, H., Keller, H.U., Agarwal, J., A'Hearn, M.F., Angrilli, F., and 56 coauthors, On the nucleus structure and activity of comet 67P/Churyumov-Gerasimenko, *Science,* 2015, vol. 347, no. 6220, p. aaa1044-1-5. doi 10.1126/science.aaa1044

Skorov, Yu.V., Rezac, L., Hartogh, P., Bazilevsky, A.T., and Keller, H.U., A model of short-lived outbursts on the 67P/CG from fractured terrains, *Astron. Astrophys.,* 2016, vol. 593, art. ID A76. doi 10.1051/0004-6361/201628365

Taylor, G.G.T., Altobelli, N., Buratti, B.J., and Choukroun, M., The Rosetta mission orbiter science overview: the comet phase, *Philos. Trans. R. Soc., A,* 2017, vol. 375, p. 20160262. doi 10.1098/rsta.2016.0262

Thomas, P.C., Veverka, J., Belton, M.J.S., Hidy, A., A'Hearn, M.F., Farnham, T.L., Groussin, O., Li, J.-Y., McFadden, L.A., Sunshine, J., Wellnitz, D., Lisse, C., Schultz, P., Meech, K.J., and Delamere, W.A., The shape, topography and geology of Tempel 1 from Deep Impact observations, *Icarus,* 2007, vol. 187, pp. 4–15. doi 10.1016/j.icarus.2006.12.013

Thomas, P.C., A'Hearn, M., Belton, M.J.S., Brownlee, D., Carcich, B., Hermalyn, B., Klaasen, K., Sackett, S., Schultz, P.H., Veverka, J., and Bhaskaran, S., The nucleus of Comet 9P/Tempel 1: shape and geology from two flybys, *Icarus,* 2013, vol. 222, pp. 453–466. doi 10.1016/j.icarus.2012.02.037

Thomas, N., Sierks, H., Barbieri, C., Lamy, P.L., Rodrigo, R., Rickman, H., Koschny, D., Keller, H.U., Agarwal, J., A'Hearn, M.F., and 51 coauthors, The morphological diversity of comet 67P/Churyumov-Gerasimenko, *Science,* 2015, vol. 347, no. 6220, p. aaa0440-1-6. doi 10.1126/science.aaa0440

*Translated by E. Petrova*